

Smart Beam Management for Vehicular Networks Using ML

G. Bharath-Reddy ⁽¹⁾, L. Montero ⁽¹⁾, J. Perez-Romero ⁽¹⁾, J. Molins ⁽²⁾, M. Ferrando-B ⁽²⁾, J. Molina ⁽³⁾, J. Romeu ⁽¹⁾, L. Jofre-R ⁽¹⁾.

bharath.reddy.ganugapanta@estudiant.upc.edu, luca.montero@upc.edu, jorperez@tsc.upc.edu, jaimoben@teleco.upv.es, mferrand@com.upv.es, josemaria.molina@upct.es, romeu@tsc.upc.edu, luis.jofre@upc.edu

(1) Universitat Politècnica de Catalunya, (2) Universidad Politécnica de Valencia, (3) Universidad Politécnica de Cartagena

Abstract- The mmWave frequencies will be widely used in future vehicular communications. At these frequencies, the radio channel becomes much more vulnerable to slight changes in the environment like motions of the device, reflections or blockage. In high mobility vehicular communications the rapidly changing vehicle environments and the large overheads due to frequent beam training are the critical disadvantages in developing these systems at mmWave frequencies. Hence, smart beam management procedures are desired to establish and maintain the radio channels. In this paper, we propose that using the positions and respective velocities of the vehicles in the dynamic selection of the beam pair, and then adapting to the changing environments using ML algorithms, can improve both network performance and communication stability in high mobility vehicular communications.

I. INTRODUCTION

Waves propagating in the mmWave band suffer from increased path loss and severe channel intermittency, and even changing the orientation of the vehicles relative to the base station can lead to a rapid drop in signal strength [1]. To deal with these impairments, vehicular networks must be provided by a set of mechanisms in which Vehicle to Infrastructure (V2I) radio channels are established by high-directional transmission links typically using high-dimensional phased arrays to benefit from the resulting beamforming gain and to maintain acceptable communication quality. These directional radio links require precise alignment of the transmitter and receiver beams, which is achieved through a series of operations known as beam management procedures. They are essential to perform various control tasks including (i) Initial access (IA) [2] for inactive users, which allows vehicles to establish a physical link connection with the Infrastructure, and (ii) Beam tracking for connected users [3], which enables beam adjustment schemes and can trigger handover procedures, route selection and recovery of radio link failures. However, directionality can significantly delay access procedures and make performance sensitive to beam alignment. These are particularly important issues in vehicular networks and motivate the need to extend current practices to innovative smart beam management methods using machine learning algorithms.

II. 5G FRAME STRUCTURE FOR TRACKING UE

The cell search is a process on the User Equipment (UE) side that is responsible for finding cells around the location of the UE. This is done thanks to the processing of the so-called Synchronization Signal block (SSB), a structure that consists of a Primary synchronization signal (PSS), a Secondary synchronization signal (SSS), and finally Physical broadcast channel (PBCH) blocks. The SSB's are grouped into the first 5 ms of an SS burst [4] and are transmitted by a gNodeB (gNB) with a configurable periodicity T_{SS} [5] with {5,10,20,40,80,160}ms intervals. Moreover, UE assumes a default periodicity of 20ms [6] during initial cell search or idle mode mobility. Fig. 1 shows the time and frequency structure of an SSB. Note that time and frequency are defined in terms of OFDM symbols and subcarriers. In a slot of 14 symbols, there are two possible locations for SSB's: symbols 2–5 and symbols 8–11.

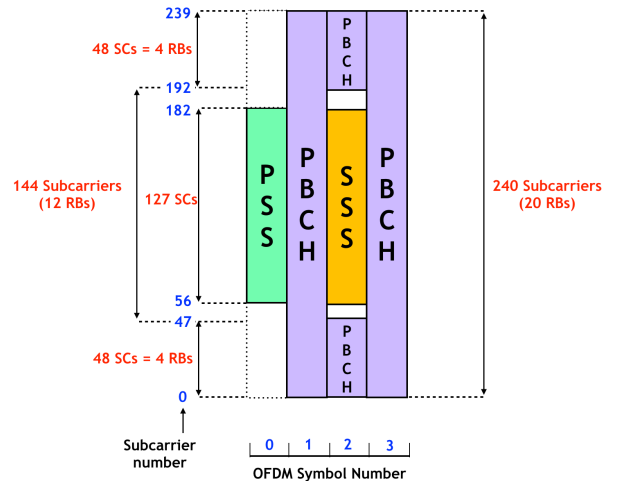


Fig. 1. SSB frame structure

The maximum number of SSB's (N_{SSB}) in a burst is frequency-dependent and is configured between $N_{SSB} \{4, 8, 64\}$ [6] and at mm-wave frequencies, there could be up to 64 blocks per burst. When considering frequencies for which beam operations are required, each SSB can be mapped to a certain angular direction which reduces UE's processing power/time

for cell search. And the subcarrier spacings (SCS) associated with each band are clearly defined by 3GPP. The SSB's occupy 20 Resource Blocks (RB) and there are 12 subcarriers in each RB, so there are a total of 240 subcarriers. Hence, the bandwidth occupied by a single SSB is 240 times the SCS. At mmWave frequencies, SCS considered for IA are 120 and 240 kHz, thus out of 400 MHz per carrier (total channel bandwidth (BW)), the bandwidth reserved for the SSB's would be respectively 28.8 MHz and 57.6 MHz [3] respectively. Given that 240 subcarriers are allocated in frequency to an SSB, the remaining bandwidth in the symbols which contain an SSB is $BW - 240 \times SCS$. Therefore, it is possible to either allocate the remaining bandwidth as shown in Fig. 2 for data transmission towards users or the information in the first 240 subcarriers i.e SSB is repeated in the remaining subcarriers to enhance the detection capabilities for high mobility users. And there are guard band intervals in frequency among the different repetitions of the SSB.

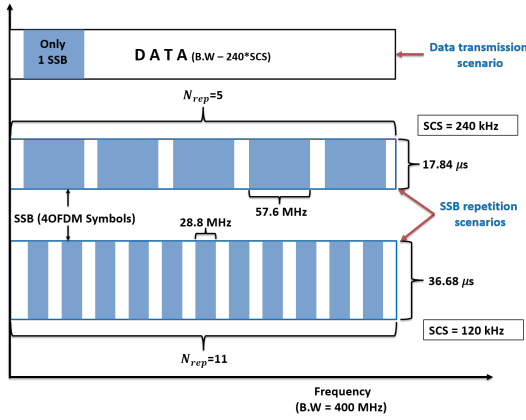


Fig. 2. Data transmission and SSB Repetition scenarios

III. EXPENSE OF OVERHEAD ON HIGH MOBILITY VEHICULAR TRACKING

Narrow beams are key to establishing highly directional radio links which are desired for mmWave vehicular communications. However, they are limited to low mobility users, because vehicles moving at high speeds could suffer from a precise alignment of transmitter and receiver beams. So, to avoid beam pointing errors, the vehicle must always be in the radiation footprint (Rad_{ft}) of the gNB where the Rad_{ft} is expressed as a function of beamwidth and radial or relative distance (R_d) as represented in equation 1.

$$Rad_{ft} = \Delta\theta_{3dB} R_d \quad (1)$$

The gNB estimates the new position of a vehicle every T_{SS} period and if the moving vehicle position is correctly estimated then it falls in the radiation footprint. Hence, to be correctly estimated by gNB, the limits on vehicular velocities (V_{veh}) are calculated by equation 2 as a function of radiation footprint and SSB burst periodicity.

$$V_{veh} < Rad_{ft}/T_{SS} \quad (2)$$

Using equation 2 we calculated the maximum limits on vehicular velocities for which $N\{16,32,64\}$ elemental antenna

array could be able to establish radio channel during IA procedure whereby default T_{SS} is 20ms and plotted on Fig. 4.

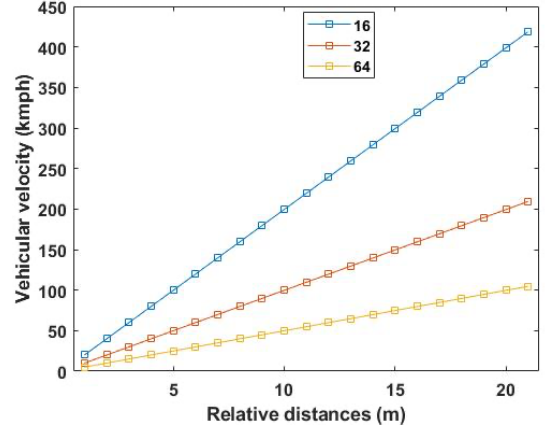


Fig. 4. Velocity as a function of relative distances, that can be processed by different N-elemental arrays during the IA procedure

Moving from idle to connected mode mobility, if the gNB configures SSB burst periodicity of 5ms for better estimating the high mobility vehicles, it comes with the expense of high overhead. We characterize this overhead (ρ) for IA and beam tracking in terms of the ratio between the total time and frequency resources R_{total} that are allocated to SSBs with the duration of the SSB burst, or the entire T_{SS} interval.

$$\rho = \frac{R_{total}}{T_{SS}BW} \quad (3)$$

Where the R_{total} is scheduled for the transmission of N_{SSB} , each spanning 4 OFDM symbols and 240 (or multiple of 240) subcarriers

$$R_{total} = N_{SSB} 4T_{OFDM} 240N_{rep} SCS \quad (4)$$

T_{OFDM} is the OFDM symbol time and is expressed in μs . From equation 4 we could observe that overhead varies with the number of SSBs per burst (N_{SSB}) and SSB burst periodicities (T_{SS}) configured by gNB. Fig. 5 shows the increasing N_{SSB} per burst can result in a large overhead.

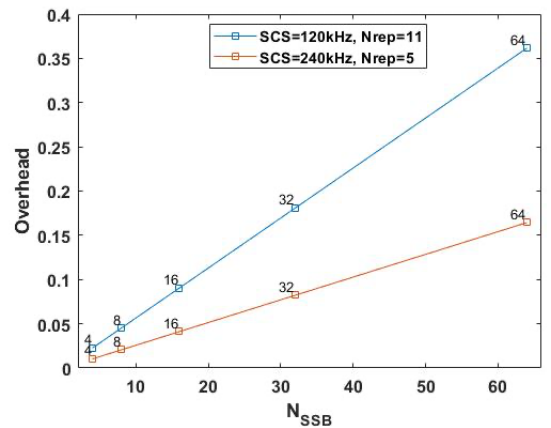


Fig. 5. Overhead as a function of N_{SSB} for different SCS and T_{SS} is set to 5ms

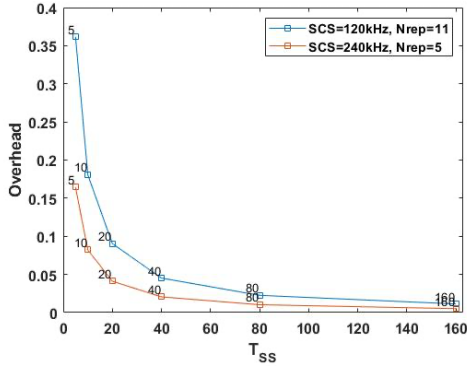


Fig. 6. Overhead as a function of T_{SS} for different SCS and N_{SSB} is set to 64

Fig. 6 shows the dependency of the overhead for tracking procedures with T_{SS} , which follows an inverse proportionality law. In particular, for very small T_{SS} (i.e., 5 ms) the impact of the SSB's with repetitions in frequency is massive, with up to 43% of the resources allocated to the SSB's. For $T_{SS} = 20$ ms or higher, instead, the overhead is always below 10%. Hence, the design and configuration of efficient IA and beam tracking procedures are of extreme importance in vehicular networks operating at mmWaves. In this paper, we propose that knowing the Global Positioning System (GPS) location of vehicles and their velocities before they arrival at a cell, can help the gNB to decide the beamwidths based on antenna array architectures to be used for the completion of the beam sweeping and reporting procedures in a single burst, so that it is possible to increase T_{SS} (e.g., to 20 or 40 beams), and reduce the overhead.

IV. NUMERICAL RESULTS

In this paper, we used a 32x 32 elemental Uniform planar array (UPA) to study the beam management procedures in different vehicular mobility scenarios and used an open-source traffic simulation package called Simulation of Urban Mobility (SUMO) for realistic traffic simulation data [7]. The SUMO simulation output file consists of the vehicular types (car, bus, etc.), their IDs, and respective GPS positions at every time step. The simulation gives 45 minutes of traffic data and the GPS positions of vehicles are noted every 100 ms.

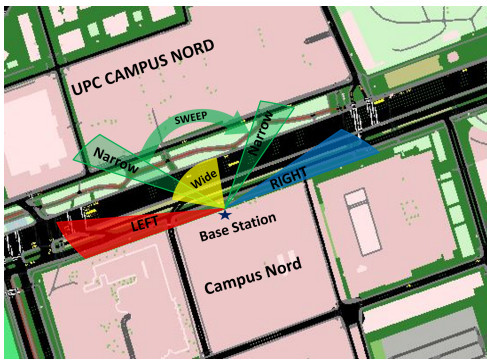


Fig. 7. Beam Management Zones

This data is then processed to extract 3 feature vectors. The decision boundaries to group the data into different clusters were set based on the conditions to reduce the overhead in high

mobility and to establish directional links in low mobility scenarios. These conditions are formulated based on the relation between vehicular velocities and their relative distances from the base station for a 32x32 UPA as shown in Fig.4. and they are defined as follows: 1) Vehicles moving closer to base station with high velocities are allocated wide beams or lower elemental array configurations 2) Vehicles moving at lower speeds are associated with narrow beams or higher array configurations and finally 3) Vehicles entering from acute left or right to the base station are assigned with a cosecant pattern as shown in Fig.8 which have small secondary lobes towards ground, so the errors from the ground reflection are minimized.

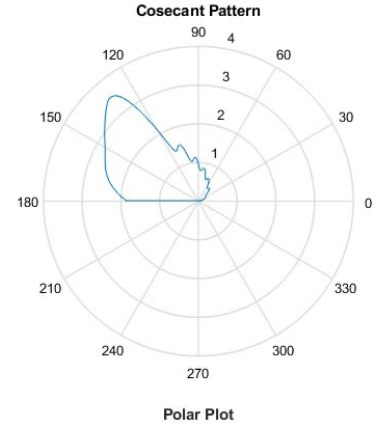


Fig. 8. Cosecant Pattern

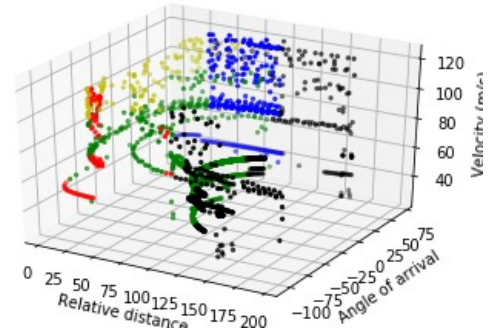


Fig. 9. 3D scatter plot

Fig. 9 is a 3D scatter plot between relative distances, velocities, and Angle of arrival (AOA) of vehicles to the base station that showcases different clusters based on the decision boundaries. The yellow data points in the scatter plot are defined from condition 1 that represents a wide beam. And the green data points in the plot are defined from condition 2 that represents a narrow beam. Whereas left and right data points are defined from condition 3 which represents the cosecant pattern beams. Finally, the black data points in the figure represents that there are beyond the range of serving cells. To further clarify the conditions explained above in Fig.4 and Fig.9 for beam assignment, a vehicle moving at a speed of 100 kmph and driving in a lane within the relative distance of 12m or less from the base station is assigned with the wide beam. Whereas, a vehicle with the same speed driving in a lane farther than 12m is allocated with the narrow beam.

To better represent and for better understanding of the clusters, a 2D plot, Fig. 10, a top view of the scatter plot in Fig. 9 between the AOA in the y-axis and relative distance from a base station in the x-axis is created.

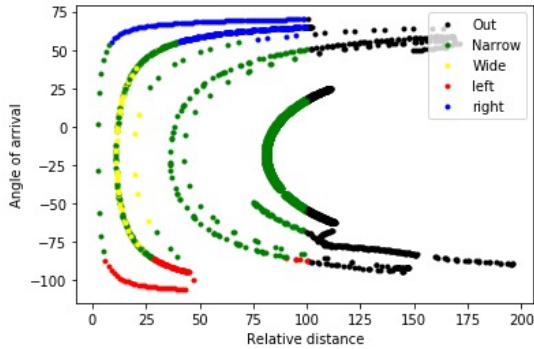


Fig. 10. 2D plot between angle of arrival and relative distance form base station

This information is used to train the Kernel Nearest Neighbors (KNN) algorithm [8][9] to implement the beam patterns for vehicular channels as discussed above. The KNN algorithm is used to predict new data based on the above-mentioned decision boundaries. This KNN algorithm shows 99% accuracy in detecting the 1) high mobility vehicles and assign them wide beam widths, 2) vehicles arriving from left and right corners of the base station and allocate the cosecant pattern, and 3) assigning narrow beams for low mobility users. Further information about the performance metrics [10] of the KNN algorithm for each condition or cluster is shown in Fig.11.

	precision	recall	f1-score	support
Narrow	0.99	0.99	0.99	720
Out	0.99	0.99	0.99	336
Wide	0.70	0.88	0.78	8
left	0.88	0.93	0.90	15
right	0.93	0.99	0.96	67
accuracy			0.99	1146
macro avg	0.90	0.95	0.92	1146
weighted avg	0.99	0.99	0.99	1146

Fig. 11. Classifier evolution metrics

Finally, the detailed breakdown of the beam allocation process for vehicular networks using ML is shown in Fig.12.

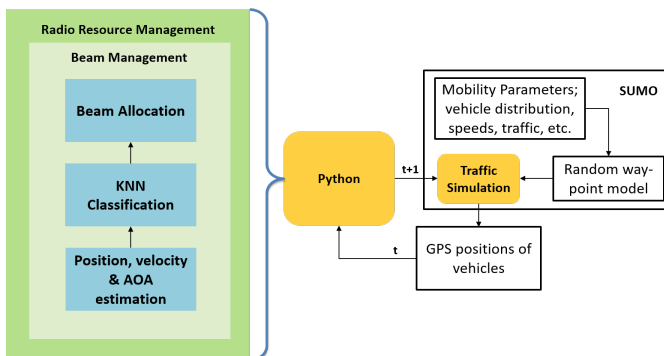


Fig. 12. Block diagram of smart beam management procedure

By this classification of vehicular traffic using KNN, we can assign the best beam pairs to vehicles in high mobility scenarios which in turn reduces, misalignment errors during the IA procedure in idle mode mobility and frequent overhead usage to maintain the connectivity in connected mode mobility.

V. CONCLUSIONS

mmWaves are widely studied to enhance the capacity of future vehicular networks. However, their performance depends on the precise beam alignment between the vehicle and the network. In this paper, we proposed a KNN based machine learning approach to solve the beam management problem by leveraging the information about the vehicle's mobility before it arrives at the base station. This approach also incurs a considerable reduction of beam tracking overhead. Finally, the benefits of our proposal are particularly useful for the high mobility vehicular use cases envisioned for 5G and beyond.

ACKNOWLEDGEMENTS

This work was supported by the Spanish "Comision Interministerial de Ciencia y Tecnologia" (CICYT) under projects TEC2016-78028-C3-1-P and MDM2016-O6OO, Catalan Research Group 2017 SGR 21, and "Industrial Doctorate" programme (2018-DI-084) of Generalitat de Catalunya.

REFERENCES

- [1] V. Raghavan et al., "Statistical blockage modeling and robustness of beamforming in millimeter wave systems" in arXiv preprint arXiv: 1801.03346, 2018.
- [2] M. Giordani, M. Mezzavilla, C. N. Barati, S. Rangan and M. Zorzi, "Comparative analysis of initial access techniques in 5G mmWave cellular networks", *Proc. Annu. Conf. Inf. Sci. Syst. (CISS)*, pp. 268-273, 2016.
- [3] M. Giordani and M. Zorzi, "Improved user tracking in 5G millimeter wave mobile networks via refinement operations", *Proc. 16th Annu. Mediterr. Ad Hoc Netw. Workshop (Med-Hoc-Net)*, pp. 1-8, Jun. 2017.
- [4] 3GPP, TS 38.211, "NR—Physical Channels and Modulation—Release 15, V15.0.0", 2018.
- [5] 3GPP, TS 38.331, "NR—Radio Resource Control (RRC) Protocol Specification—Release 15", 2018.
- [6] 3GPP, TS 38.213, "NR—Physical Layer Procedures for Control—Release 15", 2018.
- [7] D. Krajzewicz, J. Erdmann, M. Behrisch, and L. Bieker, "Recent development and applications of SUMO - Simulation of Urban MObility," *International Journal On Advances in Systems and Measurements*, vol. 5, no. 3&4, pp. 128–138, Dec. 2012.
- [8] A. Geron, 'Hands-On Machine Learning with Scikit-Learn and TensorFlow: Concepts, Tools, and Techniques to Build Intelligent Systems. O'Reilly Media, 2017.
- [9] Cover TM, Hart P (1967) Nearest neighbor pattern classification. *IEEE Trans Inf Theory* 13(1):21–27
- [10] D. M. Powers, "Evaluation: from precision, recall and Fmeasure to ROC, informedness, markedness and correlation," *Journal of machine learning research*, vol. 2, no. 1, 2011, pp. 37– 63.